Egyptian Journal of Veterinary Sciences

https://ejvs.journals.ekb.eg/

Pathological and Biochemical Studies on Hepatorenal Syndrome Induced by Bile Duct Ligation in Albino Rats

Nada N. Khalil [1*], Walaa F. Awadin [1], Alaa Samy [2] and Ahmed F. El- Shaieb [1,3]

[1] *Department of Pathology, Faculty of Veterinary Medicine, Mansoura University, Mansoura, Egypt.*

[2] *Department of Surgery, Anaesthesiology and Radiology, Faculty of Veterinary Medicine, Mansoura University, Mansoura, Egypt.*

[3] *Department of Pathology, Faculty of Veterinary Medicine, Egyptian Chinese University, Cairo, Egypt.*

Abstract

HEPATORENAL SYNDROME (HRS) is a form of secondary renal failure that occurs in late stage of chronic liver diseases. Its importance arises from the fact that it has the lowest survival rate. This study aimed to investigate the therapeutic role of Lactoferrin (LF) against the complications of hepatic fibrosis associated with bile duct ligation (BDL) in the HRS rat model. The experiment was performed on 36 adult male Sprague-Dawley rats weighting (250 - 300 gm) and their age ranged from (5-6) weeks. Rats were randomly distributed into four groups, (G1; Control normal group, n=6): rats received a daily oral dose of distilled water at (100 ml / kg/ b.wt.) for 4 successive weeks, (G2; LF group, n=6): rats received a daily oral dose of Lactoferrin at (300 mg / kg / b. wt.) by oral gavage for 4 successive weeks, (G3; BDL group, n=12): the common bile duct was double ligated, and (G4; BDL+ LF group, n=12): the common bile duct of the rats was double - ligated and then treated with LF by oral gavage from the 2nd day post -surgery and continued for 4 successive weeks . The current study recorded that LF treatment showed improvement in the clinical signs, biochemical analysis, histopathological examinations, and electron microscopy examination of the liver, kidneys, and of BDL rats compared- to the untreated BDLgroup.LF plays an important role in the treatment of hepatic fibrosis and associated complications including HRS through its antioxidant properties.

Keywords: BDL, Fibrosis, Hepatorenal Syndrome, Lactoferrin, Rat.

Introduction

Hepatorenal syndrome (HRS) is a multiorgan state characterized by hepatic and renal impairment [1]. This particular kind of functional renal failure (RF) is seen in end-stage liver disease (ESLD), such as acute liver failure (ALF), alcoholic hepatitis, and decompensated cirrhosis [2]. Based on the degree of the illness, there are two clinical forms of HRS: type I and type II. Compared to type II HRS, which has gradually growing renal retention characteristics, type I HRS is characterized by rapid development with a bad prognosis. Serum creatinine levels double in two weeks in type I patients. Two weeks following diagnosis, the death rate for patients with Type I HRS is 50%, and within months, it can reach 100% [3, 4]. A history of hepatic failure, elevated blood creatinine levels, and the lack of other renal failure causes, such as bacterial infection, shock, or nephrotoxic agent usage, as well as the absence of renal parenchymal disorders, all are necessary for the diagnosis of HRS [5].

Cholestatic liver injury is a major contributing factor to the development of hepatic fibrosis and cirrhosis, as in the case of chronic liver illness patients [6]. Experimental models were designed to simulate various features of interrelated mechanisms leading to hepatic inflammation, fibrosis, and finally cirrhosis [7]. Surgical BDL is a significant experimental paradigm utilized to generate obstructive cholestatic damage in rodents [8]. Bile acid build-up could trigger fibrotic mechanisms, either directly or indirectly, under the effect of inflammatory mediators [9].

One member of the transferrin family, the iron-binding glycoprotein, Lactoferrin (LF), is found in neutrophils, serum, and exocrine secretion [10, 11]. Saliva, tears, breast milk, and the biliary tracts are exocrine secretions containing LF, a siderophilic protein with two iron-binding sites. Colostrum has

*Corresponding authors: Nada N. Khalil, E-mail: nada43158@gmail.com, Tel.: 01060203106
(Received 15 August 2024, accepted 10 December 2024)
DOI: 10.21608/EJVS.2024.312285.2318

the highest levels of LF (5–7 mg/mL) [12]. Preceding studies had reported the multi-pharmacological characteristics of LF, including its ability to fight against bacterial and parasite infections as well as its anticancer, immunomodulatory, and anti-inflammatory actions [10, 13]. Because of its previously reported capacity to bind iron, which is believed to have oxidative features in high concentrations, LF may offer protection against oxidative stress [14]. According to the available researches, LF is extremely efficient in minimizing the concentration of cytotoxins H_2O_2 and elevating ferric- reducing antioxidant power (FRAP), both intracellularly and extracellularly [15]. LF 's ability to suppress neutrophils' "oxygen explosion," which causes a huge quantity of free radicals to be produced that harm cells, has been demonstrated to be an additional antioxidant function [16].

Since it can directly adjust immune cells' (including lymphocytes and macrophages) production of cytokines, via receptor-mediated signaling pathways, LF has also been shown to have anti-inflammatory properties [17]. Additionally, LF can reduce inflammatory reactions by inhibiting free radical damage catalyzed by iron at inflammation areas [18].

In the context of the liver, LF demonstrated direct cytoprotective action through its anti-oxidant function, inhibiting hepatocellular necrosis [19]. LF has also been shown to have a strong anti-inflammatory action, which prevents the stimulation of Hepatic stellate cells (HSCS) [20]. On the other hand, it promoted HSC apoptosis by triggering the production of macrophages, CD8+ T lymphocytes, and natural killer cells [21]. Of note, the actual LF role against hepatic fibrosis hasn't been explained till now. However, its anti-inflammatory, anti-oxidant, and proapoptotic properties could suggest an anti-fibrotic effect [22].

Material and Methods

Laboratory animals

This experiment was carried out on 36 adult male Sprague-Dawley rats, 5-6 weeks old, their weight ranged from 250g- 300g. The animals were obtained from the Medical Experimental Research Center (MERC), Faculty of Medicine, Mansoura University. Animals were left one week in the new environment in Pathology Lab, as an adaptation period before the start of the experiment. The animals were placed in plastic cages (six rats /cage), supplied with a standard pellet rat diet and water *ad libitum*, and maintained under standard human and hygienic conditions of temperature, humidity and light with a 12 h light / dark cycle.

Drugs and chemicals

Lactoferrin was purchased from Hygint pharmaceuticals (Smouha, Alexandria) in the form of powder, under the commercial name (Pravotin). It was dissolved in saline. ketoprofen was purchased from Amriya Pharm. IND. (Alexandria, Egypt). Ketamine HCl was purchased from Troikaa pharmaceuticals Ltd, Gujarat, India, under the commercial name (Ketamax 50mg/ml). Xylazine Hcl was purchased from ADWIA, Egypt, under the commercial name (Xylaject 20mg/ml).

Experimental design

Rats were divided into 4 groups. Group 1(G-1; control normal group; n = 6), rats received a daily oral dose of distilled water via oral gavage at (100 ml/kg/b. wt.) for 4 weeks. Group 2 (G-2; Lactoferrin (LF) group; n = 6), rats received a daily oral dose of Lactoferrin (LF) by oral gavage at (300 mg/kg/b. wt.) [13] for 4 successive weeks. Group 3 (G-3; BDL group; n = 12), rats undergo surgery for common bile duct ligation (CBDL). Group 4 (G-4; BDL + LF group; n = 12), rats undergo CBDL and are treated with a daily oral dose of LF at (300 mg /kg/ b. wt) via oral gavage for 4 successive weeks, started from the 2nd day post- surgery.

Surgical procedures

Anesthesia:

Isolation of *Streptococcus pyogenes* bacteria and others species as a primary step was done using blood agar. Gram stain and biochemical tests will identify the bacteria. This was done according to Quinn *et al*. [21].

Surgical procedures:

Surgery was carried out under sterile environmental conditions. An abdominal midline incision was used to expose the common bile duct guided by the xiphoid cartilage. The common bile duct was identified and then double ligated using the stomach approach technique as performed by Elsaied et al., 2020 [24]. Double ligation of the bile duct was conducted using 5-0 size polypropylene suture material without dissection in-between. Then all the abdominal organs were placed back into their normal position, and the peritoneal cavity was washed with 0.9% Sodium Chloride (NaCl) solution. The abdomen was closed in two layers: Firstly, the wall was closed by monofilament absorbable suture (Maxon 4-0), then the skin closure was done by using monofilament non-absorbable suture (Prolene 2-0) (Fig.1). Post-surgical pain in rats was treated with ketoprofen as an analgesic (3 mg/kg) injected intramuscularly [25].

Treatment with LF:

It was isolated and enumerated on Baird Parker (BP) agar (NEOGEN/UK). The black, shiny colonies with halo zones around them were picked up for morphological examination and biochemical identification according to Moraes et al. 2021 [22].

The colonies were tested for coagulase production and catalase activity for presumptive identification.

Serum samples collection

At the end of the experiment, after 4 weeks, the rats were anaesthetized with ether anesthesia after that blood samples were collected from the orbital sinus of the eye. Serum separation took place via centrifugation of blood samples at 4000 rapid per minute for ten minutes. Then serum samples were stored at -20˚C until assessment of liver and kidney function tests.

Tissue samples collection

Rats were euthanized by cervical dislocation method; then post-mortem examinations took place. Macroscopic lesions of the liver and kidneys were examined and representative tissue specimens were collected from liver and kidneys tissues from all groups, then divided into two parts; the first one was preserved separately in 10% neutral buffered formalin for histopathological examination and the second one was preserved in glutaraldehyde (4% glutaraldehyde) for ultrastructural examinations.

Histopathology (H&E)

Tissue specimens were washed then dehydrated in ascending grades of alcohol, then cleared in xylene, and embedded in paraffin wax. Thin sections (4 µ m) were cut using a microtome, deparaffinized by xylene, and finally stained with hematoxylin and eosin (H&E). Then slides were covered by cover slides to be examined by light microscope [26].

Assessment of serum liver and kidney biomarkers

Serum liver and kidney biomarkers were measured by using Enzyme Linked Immuno Sorbant Assay (ELISA) kits. Serum alanine amino transferase (ALT), aspartate amino transferase (AST) and Alkaline phosphatase (ALP) were expressed as (U/L), serum albumin was expressed in (g/dl), while serum Creatinine (SCr), total (TBIL) and direct bilirubin (DBIL) and Blood urea nitrogen (BUN) was expressed as (mg /dl). The used kits for ALT and AST were purchased from Agappe Diagnostics [27]. The used kits for ALP were purchased from Biomed Diagnostics [28]. While the kits used for BUN, Cr, TBIL, DBIL and albumin were purchased from Diamond Diagnostics [29].

Transmission electron microscopy

The liver and kidney tissue samples were cut into 1 mm^3 blocks and fixed in 2.5% glutaraldehyde (GA) and formaldehyde (FA) for 1 hour, rinsed three times in 0.075M sodium potassium phosphate buffer (pH = 7.4) for 15 min each before the samples were placed in the secondary fixative, a 1% osmium tetroxide solution for 1 hour. Following fixation, the tissue samples were rinsed again as described above. The tissues were then dehydrated in 30, 50, 70, 90%, and three changes of 100% ethanol. The samples were embedded in resin and ultrathin sections (70– 100 nm) were cut with a diamond knife using an ultramicrotome. Samples were contrasted with uranyl acetate for 5 min followed by 2 min of contrast with lead citrate, after which the samples were allowed to dry for a few minutes before being examined with the JEOL TEM (JEM 2100F) [30].

Statistical analysis

Data were edited in Microsoft Excel (Microsoft Corporation). A Shapiro–Wilk test was conducted to check for normality as described by Razali and Wah [31]. The way ANOVA procedure (PROC ANOVA; SAS Institute, 2012) was used for assessing blood parameters. Multiple comparisons among means were carried out with Duncan's multiple-range test [32]. Statistical significance was accepted as $p < 0.05$.

Results

Rats in the control and LF groups were normal with normal feed intake, physical conditions, activities, and viability. Meanwhile, BDL rats showed enlarged abdomen, yellowish discoloration of the skin, ears and tails, as well as a change in the urine color to dark yellow. These signs started on the 2nd day post-surgery and persisted till the end of the experiment. While rats in BDL+LF group showed the same signs as in the BDL group at the 2nd day post-surgery but these signs disappeared 1 week after treatment. The mortality rates of the current study were calculated for each group and represented in percentage (%). The mortality rates in the control and LF groups were zero %, while the mortality rate in the BDL group was 50 %, which started on the 2nd-day post-surgery. The mortality rate in the BDL+LF group was 30%, which started on the 10th day of treatment.

Serum activities of liver enzymes ALT, AST, and ALP as well as the concentration of TBIL and DBIL were significantly higher in the BDL group than their counterparts in the control, LF, and the BDL+LF groups ($p<0.05$), non-significant differences were observed between the control group and both of LF and BDL+LF groups ($p>0.05$) (Table 1).

About blood albumin, the lowest values were detected in the BDL group and improved significantly in response to the treatments by LF and BDL+LF ($p<0.05$) (Table 1).

The higher levels of BUN and Cr were shown in the BDL treated group compared to the control and the other two treated groups ($p<0.05$), minimizing in the LF group ($p<0.05$) (Table 1).

Macroscopically, livers from control normal (G1) and LF (G2) showed normal bright brown color with normal size. Microscpically, liver sections show the

normal arrangement of hepatocytes around central veins with normal sinusoids and portal areas in control normal G1 and G2 (Fig .2).

Macroscopically, livers from the BDL (G3) group showed yellowish discoloration, congestion with a large area of hemorrhage, dark brown discoloration with decrease size, and dark brown discoloration with atrophy. Microscpically, Liver sections from G3 show marked extension of the portal area due to congestion of portal blood vessels, portal fibrosis, dilation and proliferation of bile ductules, and few mononuclear cells infiltration in the portal area. In addition, marked lobular fibrosis leads to atrophy of hepatic cords with congested sinusoids. While the macroscopic picture of livers from the BDL+LF (G4) show normal colour and size. Microscpically, Liver sections from the BDL+ LF (G4) group showed decreased portal area, mild congestion of portal blood vessels, mild portal fibrosis, decreased proliferation of bile ductules, and few mononuclear cells infiltration in the portal area (Fig .3).

Macroscopic examination of kidneys showed a normal bright brown color with normal colour and size in normal control and LF (G1 and G2) groups. Meanwhile, microscpically, kidney sections showed normal glomeruli and tubules in normal control and LF (G1 and G2) groups (Fig. 4).

Macroscopic picture of kidneys from the BDL (G3) group showed dark brown discoloration with increased size. Kidney sections from the BDL (G3) group showed congested blood vessels, prominent hemosiderosis in the tubular epithelium, dilated Bowman's space, tubular hydropic degeneration, coagulative necrosis, mild perivascular fibrosis, and perivascular edema. While the macroscopic picture of kidneys from the BDL + LF (G4) group shows a normal brown color with decreased size. Microscpically, kidney sections from the BDL + LF (G4) group showed normal tubules and dilated Bowman's space (Fig. 5).

Representative Transmission Electron Microscope (TEM) micrograph of liver sections from the control group (G1) showed intact ultrastructure of nucleus and nucleolus with abundant cytoplasmic mitochondria and RER. LF group (G2) showed the normal structure of hepatocytes (centrally intact nucleus with nucleolus and abundant mitochondria with normally arranged Rough-endoplasmic Reticulum (RER) (Fig. 6).

On the other hand, liver sections from rats of the BDL group (G3) showed shrunken nucleus with nuclear membrane blebbing and perinuclear loss of cytoplasmic organelles characterized by clumped to dilated RER, reduction of mitochondrial number with irregularity and abundant electron- dense clumped mitochondria. While liver sections from the BDL+LF group (G4) showed partial hepatic degeneration represented by few cytoplasmic dilations of RER with scattered electron-dense clumped irregularly shaped mitochondria, an intact nucleus with eccentric nucleolus (Fig. 7).

Representative TEM micrograph of kidney tubular epithelium and the glomerulus of control group (G1) tubular epithelial cells showed intact basement membrane with basal infoldings of plasma membrane and abundant cytoplasmic mitochondria with few vacuoles and partial indentation nuclear membrane. While TEM of the LF group (G2) showed intact basolateral plasma membrane infoldings with intact mitochondria beside a few cytoplasmic vacuoles (Fig. 8).

Meanwhile, the BDL group (G3) showed fused basolateral plasma membrane infoldings, shrunken nuclei with finger-like projection of nuclear membrane, abundant cytoplasmic vacuoles, and fragmented to clumped mitochondria. Meanwhile, TEM of the BDL+LF group (G4) showed blebbing of the nuclear membrane with thickening of basolateral plasma membrane infoldings and mitochondrial irregularity with electron- dense appearance with occasional cytoplasmic vacuoles (Fig. 9).

Representative glomerular ultrastructure showed in the control group (G1) glomerulus showing intact interwoven capillary loops lined with fenestrated endothelial cells, glomerular basement membrane, and many foot processes in contact with podocytes, uriniferous space are in between the capillary loop. LF group (G2) showed intact fenestrated endothelium with intact glomerular basement membrane, partial fusion of foot process with occasional nuclear pyknosis of podocytes (Fig. 10).

While the BDL+LF group (G3) shows marked disruption of glomerular structure with fragmented endothelial cells, thickened basement membrane, loss of filtration slits, closure of uriniferous space with detached foot process, and fragmented podocytes. While BDL+LF group (G4) showed partial nuclear shrunken of one podocytes with intact ultrastructure of fenestrated endothelium, GBM, and foot process with normal uriniferous space (Fig. 11).

Discussion

Different experimental models have been known to induce hepatic fibrosis [33]. But none of them went through a thorough evaluation to serve as a model for HRS [34]. The common bile duct ligation CBDL and carbon tetrachloride CCL_4 administration are the two commonly used research models of liver disease. The primary benefit of BDL is that, in comparison to the administration of CCL_4, it allows

for the study of changes in renal function over a brief period with reduced death rates [35].

LF belongs to the transferrin protein family. Where it forms robust connections with two ferric ions and presents in exocrine secretions, including tears and colostrum [13]. It had antioxidant and anti-inflammatory actions as stated by various researchers [6, 36, 37]. Moreover, LF protects hepatocytes against acetaminophen- induced toxicity as demonstrated by earlier investigations, which added to its role as a hepatoprotective agent [19]. Also, it can protect hepatocytes against dimethylnitrosamine-induced liver toxicity, as demonstrated before [38]. In a rat model of CCL_4-induced hepatitis, LF decreases IL-1β, so it prevents hepatitis [13]. Owing to its anti-inflammatory and anti-fibrotic properties, LF may also be useful in the treatment of liver fibrosis in a rat model subjected to BDL. It reduces inflammatory cytokines such as TNF-α and IL-1β while raising the anti-inflammatory cytokine IL-10 to achieve its anti-inflammatory effect[6].

In the current investigation, all rats showed jaundice from the 2nd day post-surgery indicating a successful ligation. Due to the obstruction of bile flow following CBDL and the accumulation of bilirubin on tissues, primarily the skin and mucous membranes, jaundice was thought to result from elevated blood bilirubin concentrations [39]. These findings were in consistent with [40]. Clinical signs recorded in this study agreed with other studies [41]. These could be attributed to the increase in serum levels of bilirubin causing jaundice and cystic dilation of the common bile duct due to obstruction of bile.

Significant increases in the serum levels of ALT and AST were observed in the BDL group as an indicators of liver function, which were similar to the levels in [42-44]. On the other hand, in the BDL+LF group, LF decreased the serum levels of AST and ALT near normal levels in the control and the LF groups. This finding was similar to that of [45]. This decline demonstrates the hepatoprotective effect of LF in preserving the structure and function of the liver cells [19].

The only organ where albumin is synthesized is the liver [46]. The most significant protein in plasma that the liver produces is called albumin, which can be used as a good measure of liver condition [47]. According to our study, BDL rats ' serum albumin levels decreased compared to the control group, which agreed with the results of [46, 48]. Reduced protein synthesis and hepatic dysfunction could be the cause of this drop in serum albumin content [49]. Moreover, these alterations in albumin levels could be the result of metabolic changes, including decreased liver manufacturing associated with BDL [50]. However, rats treated with LF in the BDL+ LF and LF groups showed a significant increase in serum albumin concentration. This effect could be connected to LF 's antioxidant qualities [6]. Furthermore, this rise can be the result of increased albumin and protein production, which speeds up the regeneration process and protects the liver [51].

According to the current study, Serum levels of cholestatic indices including ALP, TBIL and DBIL in the BDL group were significantly increased compared with the control group. These data are similar to the results of [43, 52]. Meanwhile, the BDL-induced hepatocyte degeneration and bile duct obstruction may be the reason for the rise in serum concentrations of TBIL and DBIL [53]. In the control and LF group, there is no change in the level of cholestatic indices. While rats treated with LF in the BDL+LF group showed a reduction in the levels of these biochemical markers as compared to the BDL group. The reduction in ALP enzyme activity indicates the functional integrity of the hepatic cell membrane and is a clear sign of hepatoprotective effect[54]. This reduction in response to treatment by LF could be due to its hepatoprotective action.

The biochemical analyses provide a more significant diagnostic tool for HRS rather than other clinical signs [39]. So, significantly high serum Blood Urea Nitrogen (BUN) and Creatinine (Cr) levels in the BDL group are the primary laboratory results associated with HRS. These findings agreed with the findings of [34, 55, 56]. The mechanism of renal failure progression in this model is following the mechanisms observed in typical HRS [57]. Damage to the liver parenchyma is the first step in the progressive process, which also includes the development of portal hypertension, splanchnic vascular bed enlargement, a decrease in the effective volume of fluid in the systemic circulation, and vascular baroreceptor stimulation. These events are followed by the activation of various vasoconstriction factors, such as the sympathetic nervous system, renin-angiotensin system, or arginine vasopressin system [57]. Renal hypoperfusion, renal cortical vasoconstriction, and renal failure (RF) are caused by these mechanisms [58]. The reduction in renal blood flow and glomerular filtration rate due to renal vasoconstriction is reflected on the biochemical profile of renal function, which includes an increase in serum creatinine and BUN levels [59].

On the other hand, rats treated with LF in the BDL+LF recorded a significant decrease in serum BUN and Cr near the normal levels present in both the control and LF groups. These results were partially agreed with [60], who recorded that LF inhibited oxidative stress-induced cell death and apoptosis in human kidney tubular epithelial cells.

This may be attributed to the hepatoprotective effect and antifibrotic actions of LF on hepatocytes [6] which in turns protects liver cells from damage and so prevents development of HRS.

A prevalent pathological characteristic of many liver illnesses is cholestasis, which causes inflammation, cirrhosis, and hepatotoxicity [61]. Hepatocyte apoptosis, the production of oxygen derivatives, and inflammation have all been demonstrated to rise in response to cholestasis-induced bile acid buildup and other toxic substances [43]. While cirrhosis and cholestasis primarily affect the liver, they can also cause damage and dysfunction to other extrahepatic organs, particularly the kidneys [62]. Two important adverse effects of acute liver failure are hepatic encephalopathy HE and HRS [2, 63].

One of the possible causes of renal dysfunction, or HRS, in hepatic failure is oxidative stress and inflammation [64]. Moreover, it has been discovered that oxidative stress may be a major factor in problems caused by cholestasis [55]. Many Researches and experiments have connected renal disease to inflammation and oxidative stress, which are caused by a variety of pathological circumstances that result in the production of harmful compounds that release free radicals. Because of their extreme reactivity, free radicals damage lipids, proteins, and nucleic acids, impairing their structural and functional integrity [64]. So, the need for an antioxidant agent to alleviate liver injury by reducing free radicals- induced tissue damage become an urgent necessity.

The gross examination of livers from the BDL group in this study was similar to the findings of [65]. The hepatomegaly seen may be due to stimulation of HSC during hepatocyte injury which causes it to transdifferentiate into myofibroblasts-like cells and form the extracellular matrix [66]. The dark brown discoloration may be due to congestion of hepatic sinusoids and inflammation, while the yellowish discoloration may be due to fibrosis.

In the current investigation, the histopathological examination of liver tissues of the BDL group were in accordance with previous investigations [39, 44, 56, 67]**.** Previous research has demonstrated that the bile duct hyperplasia seen in this investigation [68], is the earliest morphological sign of hepatic damage connected to extrahepatic bile duct blockage [69]. It remains unclear what causes this proliferative response to begin. It has been suggested that cell proliferation may be aided by the rise in intraductal pressure that results from blockage of the common bile duct [69], however the exact biochemical processes behind this pressure impact are unclear [68]. So this finding is consistent with the increase in serum levels of ALT, AST, ALP, TBIL, DBIL and albumin seen in the BDL group. High ALT level has a stronger connection with the condition of necrosis, while increased AST refers to liver damage in rats [70]. As a marker of the integrity of the liver's plasma membrane, ALP is concentrated in the bile duct cells [45]. The rise in ALP, which is a consistent indicator of hepatobiliary dysfunction caused by liver injury, occurs due to new synthesis by liver cells [71]. These alterations in liver enzyme levels point to a loss of tissue integrity, which leads to hepatocytes death and subsequent necrosis [72], showing the extent of hepatic injury in cholestasis and the toxic effects of bile acids on the liver [73].

In the BDL model, cholestasis decreases bile salt excretion, which results in the retention of hydrophobic bile salts within hepatocytes, as well as apoptosis, necrosis, and the loss of liver parenchyma, all of which contribute to a redox imbalance and the generation of reactive oxygen species (ROS) [74]. Furthermore, ROS leads to significant injury to mitochondrial DNA and the liver, degrading proteins within cells and interfering with mitochondrial production [74]. It has been discovered that oxidative stress and free radicals play a major role in the development and spread of liver damage and fibrosis [75]. Antioxidants may therefore be promising treatments for liver fibrosis and the problems associated with it [71, 76]

It was recorded that LF plays a role in the amelioration of fibrotic changes induced by BDL in a rat model [6]. The results of the current study recorded that LF significantly reduced BDL-induced liver histological alterations in rats when the treatment starts immediately after BDL in the BDL+LF group. This response to the LF treatment is attributed to its hepatoprotective and anti-oxidative properties.

The gross examination of kidneys in BDL group in this study did not agree with the previous investigations that recorded macroscopically greenish kidneys with an irregular surface in 8-week CBDL mice [77]. This difference in color might be attributed to the difference in species and long- term bile duct ligation under the effect of high serum bilirubin and bile acids.

The current study recorded congested blood vessels, tubular hydropic degeneration, coagulative necrosis, mild perivascular fibrosis, hemosiderosis in the tubular epithelium, dilated Bowman's space, and perivascular edema. The microscopic findings of this study were supported by the findings of [39, 56, 78]. Renal structural damage, including apoptosis, necrosis, and fibrosis, is caused by chronically elevated oxidative stress, renal vasoconstriction, and hypoperfusion in cirrhotic individuals with HRS-

CKD[1, 79]. Oxidative stress destroys the glomerulus [80] and the inflammation that occurred [81]. Acute renal failure may also be linked to oxidative stress [82], obstructive nephropathy [83], and inflammation that resulted in chronic renal failure [84].

Levels of serum bile and bilirubin rise in case of liver failure [85]. Proximal tubular function can be compromised by elevated serum levels of bile acids or bilirubin, a condition that resolves when the levels return to normal [86]. The primary cause of the current paradigm of renal failure in HRS is significant splanchnic and systemic vasodilation, which lowers the glomerular filtration rate [87]. But without taking into account the effect of renal bile casts, this schema is lacking [85].

Besides its anti-fibrotic properties on human renal tissue , it was found that LF prevented cell injury and then death associated with oxidative stress [60]. In this study, the tissue examination of kidneys from the BDL + LF group showed normal tubules and dilated Bowman's space compared with the BDL group. This shows that antioxidant therapy avoids renal failure and restores normal glomerular filtration rate, renal blood flow, and mean arterial pressure in cirrhotic rats, indicating that oxidative stress had an important role in all of these changes [88].

In the current investigation, ultrastructural examinations of liver sections of the BDL group using TEM showed showing shrunken nucleus with nuclear membrane blebbing and perinuclear loss of cytoplasmic organelles characterized by clumped to dilated RER, reduction of mitochondrial number with irregularity and abundant electron-dense clumped mitochondria. These results were in accordance with [88], and partially agree with [90] who recorded that the shape of the hepatocyte nuclei became irregular, and some even appeared pyknotic in the BDL group. The mitochondria partly disappeared in damaged hepatic cytoplasm, with vacuolar degeneration visible occasionally. Furthermore, the structure of the hepatic interstitial was disordered, where bile duct endothelial cells, fibroblasts, macrophages, lymphocytes and neutrophils increased. The normal structure of sinusoidal endothelial fenestrae also disappeared. This may be due to difference in time period of ligation, which was 3 weeks. On the other hands, rats belonging to the BDL+ LF group using TEM showed partial hepatic degeneration represented by a few cytoplasmic dilations of RER with scattered electron dense clumped irregularly shaped mitochondria, intact nucleus with the eccentric nucleolus. The effect of treatment with LF on the ultrastructure of the liver was not discussed in the literature before.

In the present study, the ultrastructural examinations of kidney tubular epithelium of BDL group using TEM showed fused basolateral plasma membrane infoldings, shrunken nucleus with finger like projection of nuclear membrane, abundant cytoplasmic vacuoles and fragmented to clumped mitochondria. These results disagree with that of [91] which recorded swelling and enlargement of renal tubular cells, increase in number of lysosomes containing myeloid bodies and a relative decrease in the number of mitochondria especially in the proximal tubules in the BDL group. This could be due to the long period of BDL in our study. Meanwhile the effect of treatment by LF appeared in the BDL+LF group showing blebbing of nuclear membrane with thickening of basolateral plasma membrane infoldings and mitochondrial irregularity with electron dense appearance with occasional cytoplasmic vacuoles. No literature discussed the effect of LF in BDL rats before.

BDL group showed marked disruption of glomerular structure with fragmented endothelial cells, thickened basement membrane, loss of filtration slits, closure of uriniferous space with detached foot process and fragmented podocytes. These results disagree with that of [92]. While sections of BDL+LF group showing partial nuclear shrunken of one podocytes with intact ultrastructure of fenestrated endothelium, GBM and foot process with normal uriniferous space. There has been no research discussed previously the effect of LF on ultrastructural examination of kidney sections.

Conclusion

This study illustrated that role of LF in the prevention and treatment of hepatic fibrosis and its associated complications including HRS through its potent antioxidant and anti-inflammatory actions.

Acknowledgments

We really appreciate all the staff members of Medical Experimental Research Center (MERC) who helped in the Experimental part.

Funding statements

This study didn't receive any funding support

Declaration of Conflict of Interest

There are no conflicts of interests to declare.

Ethical of approval

The experimental procedures were carried out according to the guidelines of Faculty of Veterinary Medicine, Mansoura University, and approved by the Ethical Committee in Mansoura University (Ethical code No. M/17, approved on the 8th of August, 2019).

TABLE 1. Effect of different treatments on liver and kidney functions as well as blood protein (albumin).

Items	Control	Lactoferrin	BDL	BDL+Lactoferrin	p-value
Liver function					
ALT (U/L)	61.00±5.57^{b}	52.20±8.45^{b}	116.50±10.89^{a}	54.13±4.61^{b}	<.0001
AST (U/L)	99.00±8.36^{b}	89.60±12.46^{b}	455.60±24.14^{a}	127.63±25.11^{b}	<.0001
ALP (U/L)	292.40±21.15^{b}	279.70±21.41^{b}	478.23±46.66^{a}	256.00±24.76^{b}	0.0002
T BIL (mg/dL)	0.50±0.14^{b}	0.52±0.16^{b}	6.94±1.34^{a}	0.91±0.22^{b}	<.0001
D BIL (mg/dL)	0.40±0.05^{b}	0.19±0.08^{b}	3.68±0.99^{a}	0.42±0.15^{b}	<.0001
Kidney function					
CR (mg/dL)	0.32±0.07^{b}	0.30±0.08^{b}	1.12±0.17^{a}	0.46±0.05^{b}	<.0001
BUN (mg/dL)	22.29±1.32^{b}	19.26±1.61^{b}	41.50±1.59^{a}	20.96±0.86^{b}	<.0001
Blood protein					
ALB (g/dL)	3.68±0.23^{a}	2.94±0.33^{a}	1.92±0.34^{b}	2.90±0.14^{a}	0.0021

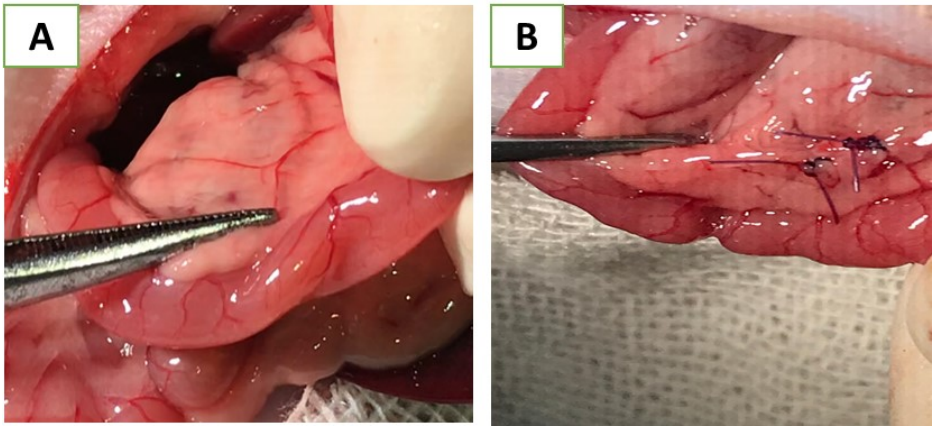

Fig. 1. (A) Identification of the common bile duct.(B) Double ligation of the bile duct using 5-0 size polypropylene suture material without dissection in-between.

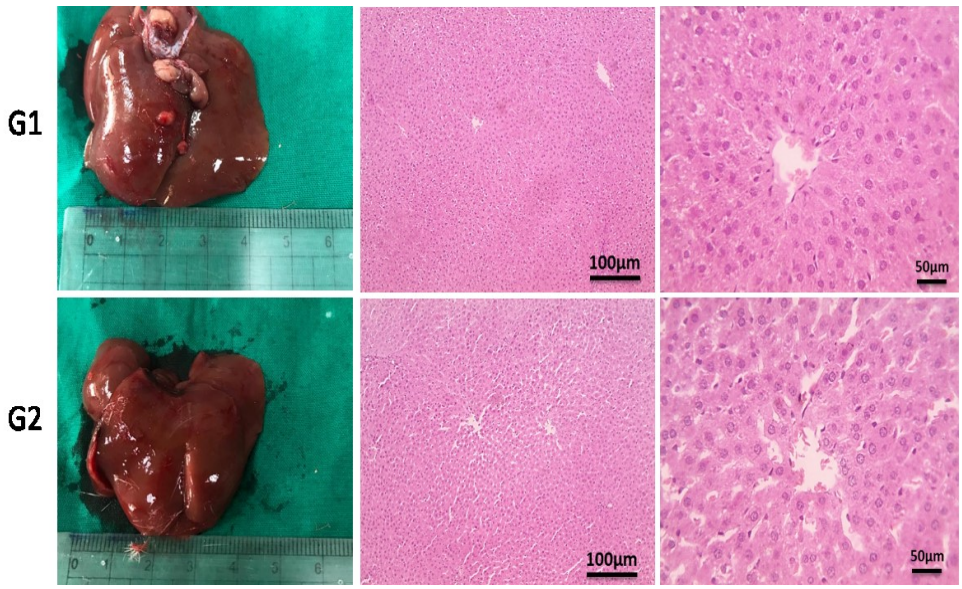

Fig. 2. Gross picture of livers showing normal bright brown color with normal size. Microscpically, liver sections showing normal arrangement of hepatocytes around central veins with normal sinusoids and portal areas in control normal G1 and G2. HE Magnifications X: 100 bar 100 and X: 400 bar 50.

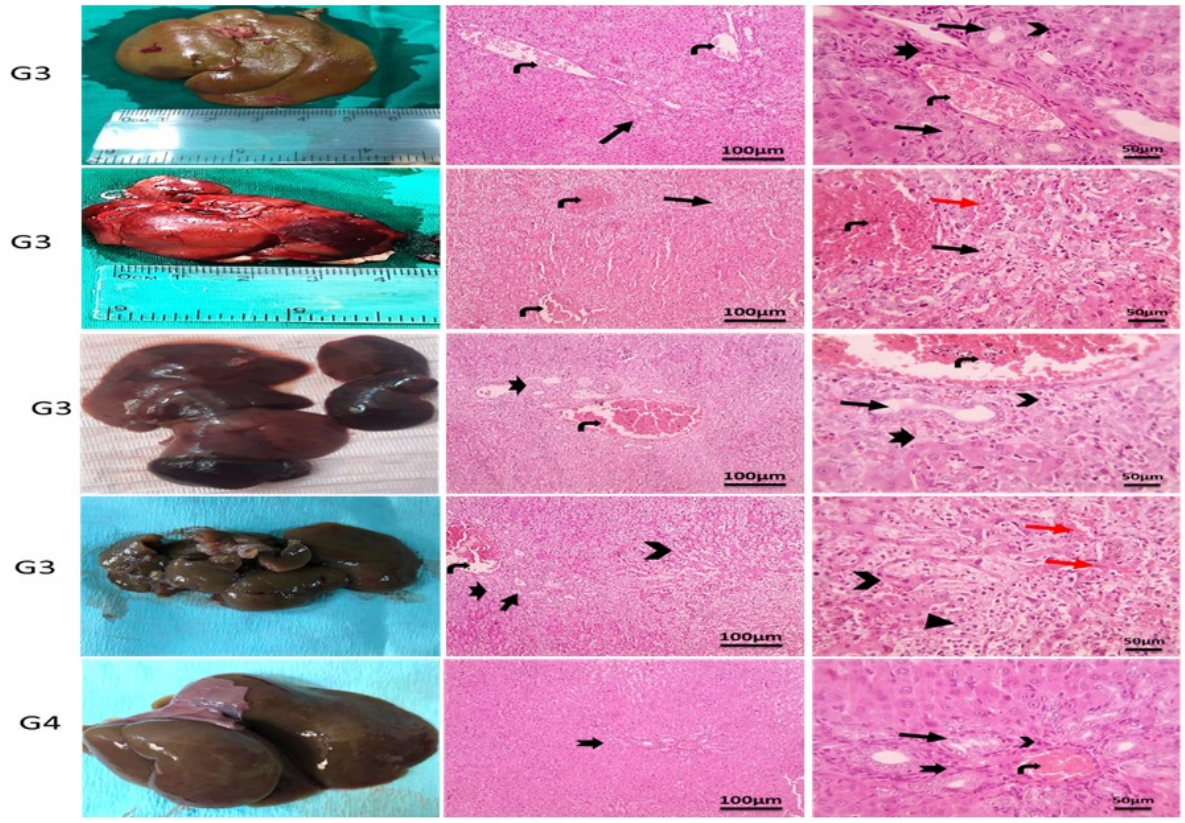

Fig. 3. Gross picture of livers from G3 showing yellowish discoloration 1st panel, congestion with large area of hemorrhage 2nd panel, dark brown discoloration with decrease size 3rd panel, dark brown discoloration with atrophy in 4th panel. Microscpically Liver sections from control +ve G3 showing marked extension of portal area due to congestion of portal blood vessels (angled black arrow), portal fibrosis (thick black arrow), dilation and proliferation of bile ductules (thin black arrow), few mononuclear cells infiltration in portal area (arrowhead). Marked extension of portal area due to congestion of portal blood vessels (angled black arrow), portal fibrosis (thick black arrow), marked proliferation of bile ductules (thin black arrow), few mononuclear cells infiltration in portal area (arrowhead). in addition, marked lobular fibrosis (closed arrowhead) leading to atrophy of hepatic cords (opened arrowhead) with congested sinusoids (red arrows). Gross picture of livers from G4 showing normal colour and size. Microscpically, Liver sections from G4 showing decreased portal area mild congestion of portal blood vessels (angled black arrow), mild portal fibrosis (thick black arrow), decreased proliferation of bile ductules (thin black arrow), few mononuclear cells infiltration in portal area (arrowhead). HE Magnifications X: 100 bar 100 and X: 400 bar 50.

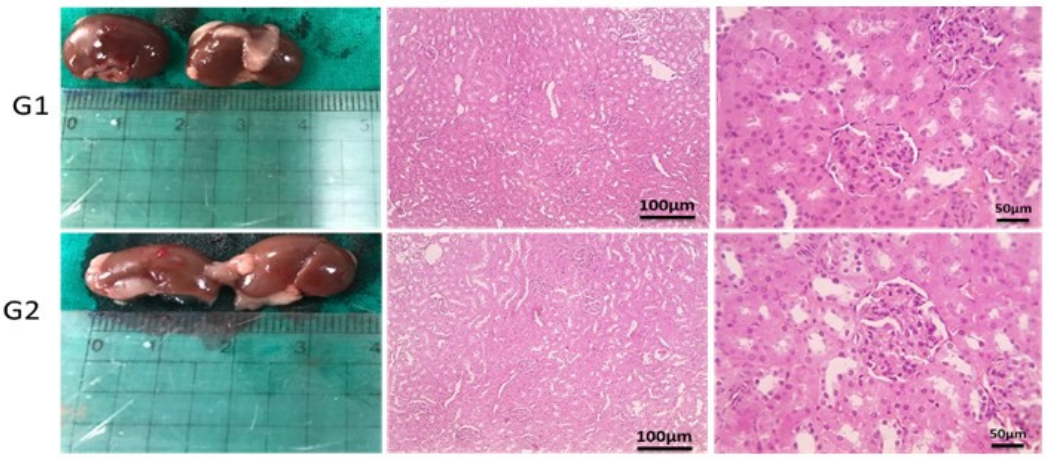

Fig. 4. Gross picture of kidneys showing normal bright brown color with normal colour and size. Microscpically, kidney sections showing normal glomeruli and tubules in control normal G1 and G2 HE Magnifications X: 100 bar 100 and X: 400 bar 50.

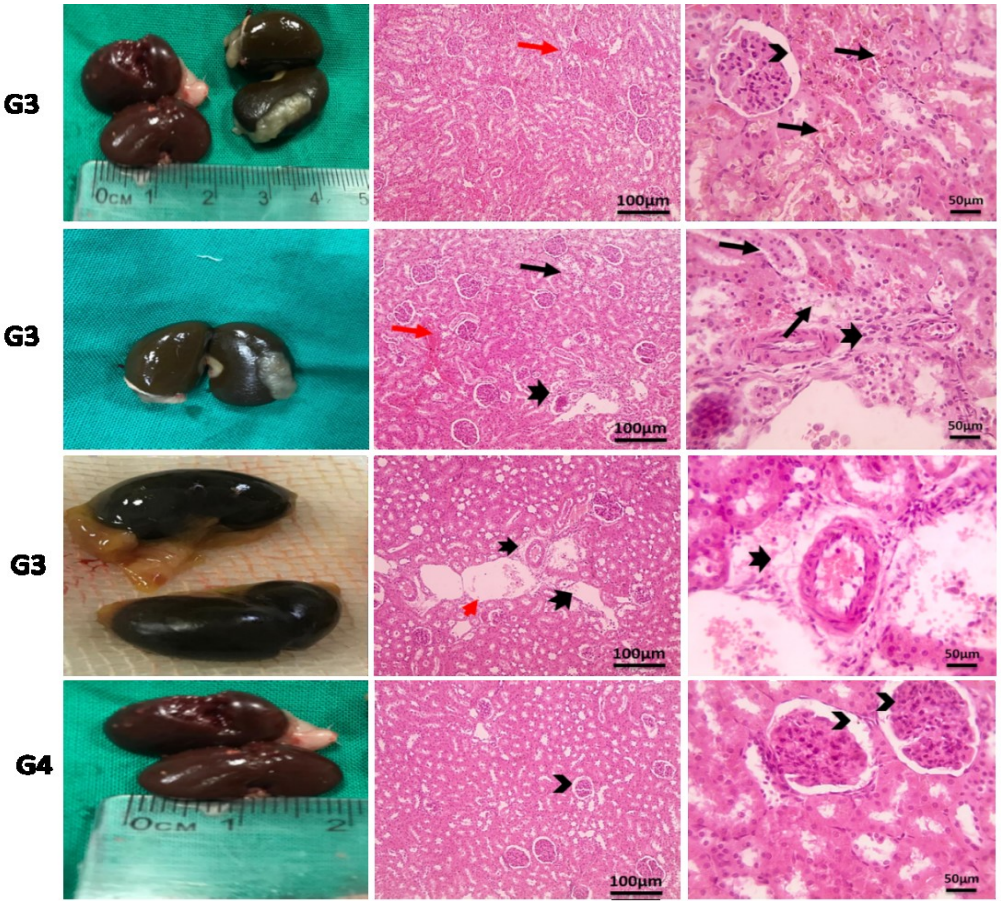

Fig. 5. Gross picture of kidneys showing dark brown discoloration color with increased size as in 3rd panel. Microscpically, kidney sections showing normal glomeruli and tubules in control normal G1 and G2. Kidney sections from G3 showing congested blood vessel (red arrow), prominent hemosiderosis in tubular epithelium (black arrow), dilated Bowman's space (arrowhead), tubular hydropic degeneration and coagulative necrosis (thin blue arrow), mild perivascular fibrosis (thick black arrow), perivascular edema (thick black arrow). Gross picture of kidneys showing normal brown color with with decreased size. Microscpically, kidney sections from G4. showing normal tubules and dilated Bowman's space (arrowhead). HE Magnifications X: 100 bar 100 and X: 400 bar 50.

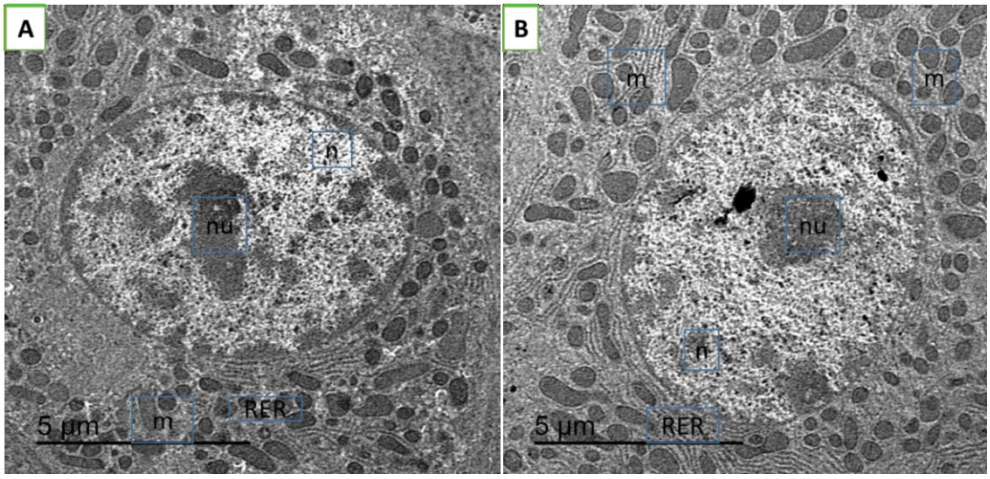

Fig. 6. Representative TEM micrograph of liver from different treatment groups. A) Control normal group (G1) showing intact ultrastructure of nucleus (n) and nucleolus (nu) with abundant cytoplasmic mitochondria (m) and RER (RER). B) LF group (G2) showing normal structure of hepatocytes centrally intact nucleus (n) with nucleolus (nu) and abundant mitochondria (m) with normally arranged RER (RER).

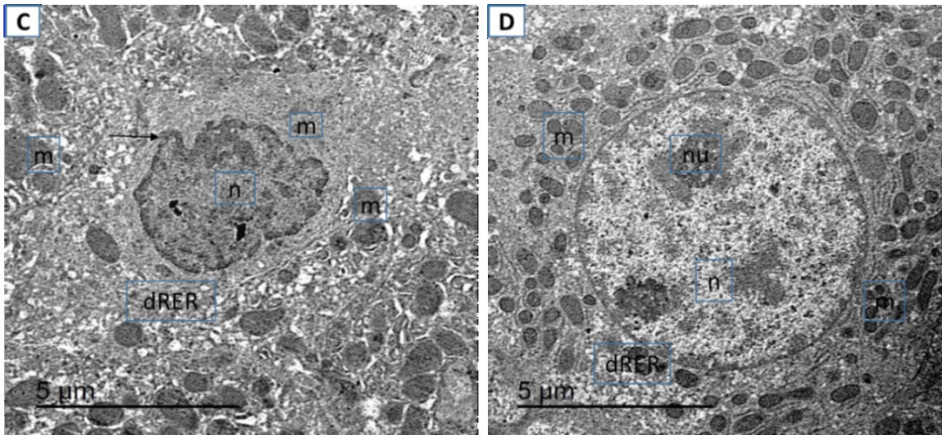

Fig. 7. C) BDL group (G3) showing shrunken nucleus (n) with nuclear membrane blebbing (thin arrow) and perinuclear loss of cytoplasmic organelles characterized by clumped to dilated RER (dRER), reduction of mitochondrial number with irregularity and abundant electron dense clumped mitochondria (m). D) BDL+LF group (G4) showing partial hepatic degeneration represented by few cytoplasmic dilations of RER (dRER) with scattered electron dense clumped irregularly shaped mitochondria (m), intact nucleus (n) with eccentric nucleolus (nu). Bar= 5 µm.

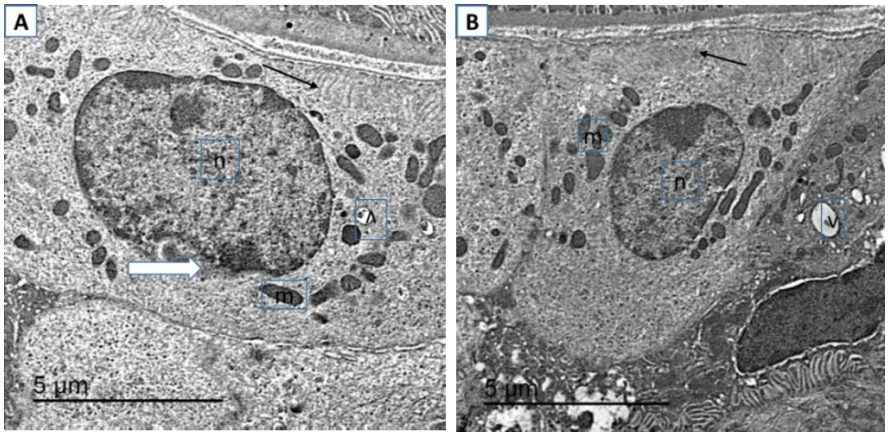

Fig. 8. Representative TEM micrograph of kidney tubular epithelium and the glomerulus from different treatment groups. A) Control normal group (G1) tubular epithelial cells showing intact basement membrane with basal infoldings of plasma membrane (thin arrow) and abundant cytoplasmic mitochondria (m) with few vacuoles (v) and partial indentation nuclear membrane (thick arrow). B) LF group showing intact basolateral plasma membrane infoldings (thin arrow) with intact mitochondria (m) beside few cytoplasmic vacuoles (v).

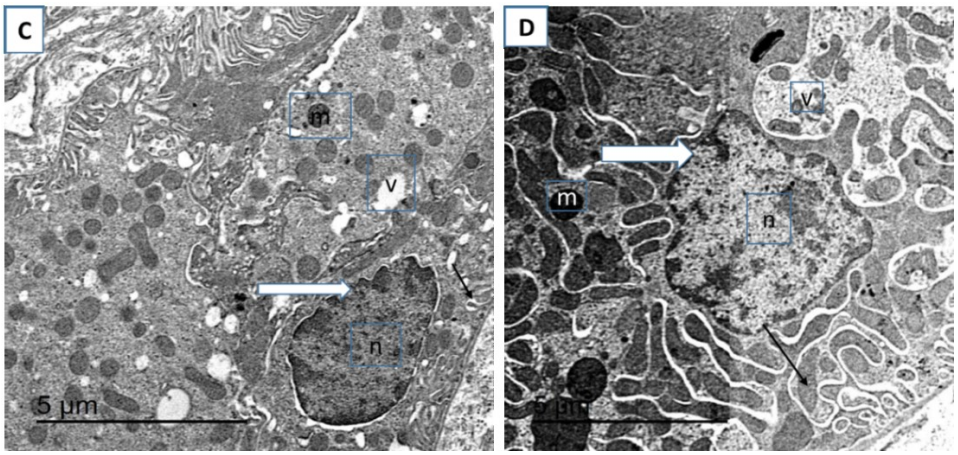

Fig. 9. C) BDL group showing fused basolateral plasma membrane infoldings (thin arrow), shrunken nucleus (n) with finger like projection of nuclear membrane (thick arrow), abundant cytoplasmic vacuoles (v) and fragmented to clumped mitochondria (m). D) BDL+LF group showing blebbing of nuclear membrane (thick arrow) with thickening of basolateral plasma membrane infoldings (thin arrow) and mitochondrial irregularity with electron dense appearance (M) with occasional cytoplasmic vacuoles (v).

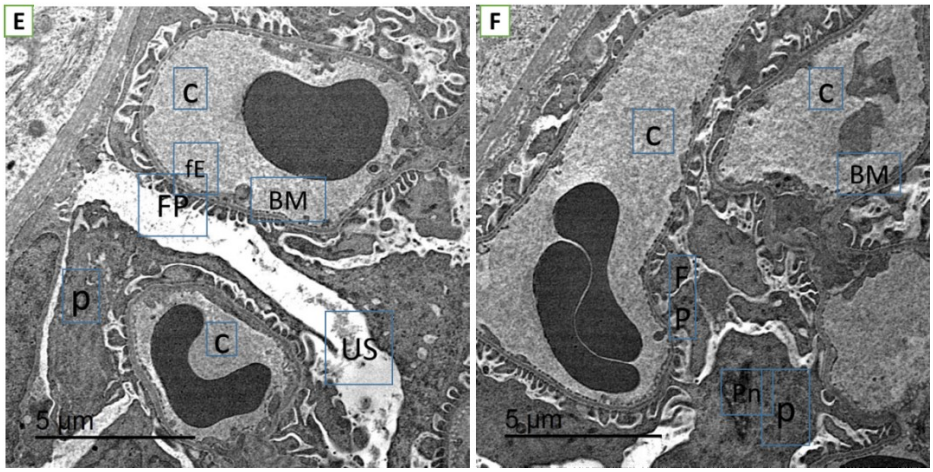

Fig. 10. Representative glomerular ultrastructure. E) Control group (G1) glomerulus showing intact interwoven capillary loops (c) lined with fenestrated endothelial cells (fE), glomerular basement membrane (BM) and many foot process (FP) in contact with podocytes (p), uriniferous space (US) are in between the capillary loop (c). F) LF (G2) group showing intact fenestrated endothelium with intact glomerular basement membrane (BM), partial fusion of foot process (FP) with occasional nuclear pyknosis (pn) of podocytes (p).

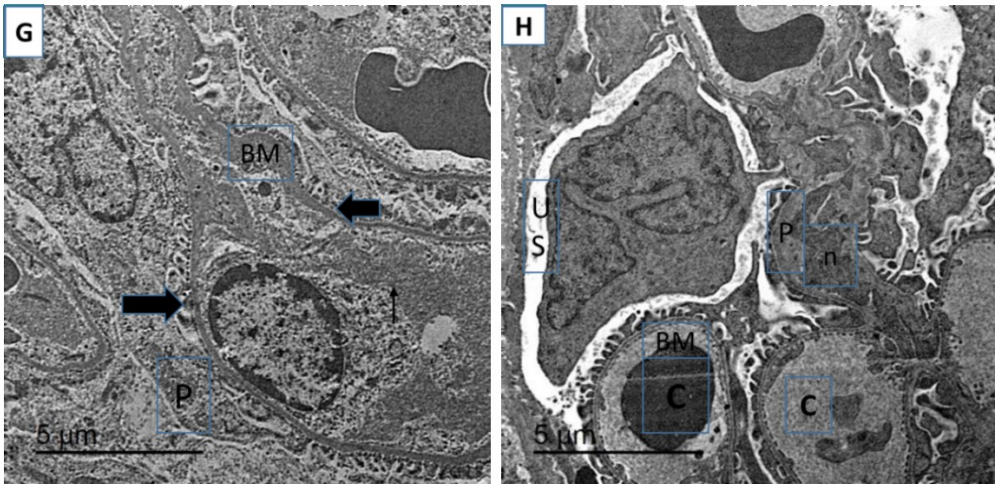

Fig. 11. G) BDL (G3) group showing marked disruption of glomerular structure with fragmented endothelial cells (thin arrow), thickened basement membrane (BM), loss of filtration slits, closure of uriniferous space with detached foot process (thick arrow) and fragmented podocytes (p). H) BDL+LF (G4) group showing partial nuclear shrunken (n) of one podocytes (p) with intact ultrastructure of fenestrated endothelium, GBM (BM) and foot process (FP) with normal uriniferous space (US). Bar= 5 µm.

References

1. Rodriguez, E., Henrique Pereira, G., Solà, E., Elia, C., Barreto, R., Pose, E., Colmenero, J., Fernandez, J., Navasa, M., Arroyo, V. and Ginès, P., Treatment of type 2 hepatorenal syndrome in patients awaiting transplantation: Effects on kidney function and transplantation outcomes. *Liver Transplantation*, **21**(11), 1347-1354 (2015).
2. Ginès, P., Guevara, M., Arroyo, V. and Rodés, J. Hepatorenal syndrome. *The Lancet*, **362**(9398), 1819-1827 (2003).
3. Alessandria, C., Ozdogan, O., Guevara, M., Restuccia, T., Jiménez, W., Arroyo, V., Rodés, J. and Ginès, P., MELD score and clinical type predict prognosis in hepatorenal syndrome: Relevance to liver transplantation. *Hepatology*, **41**(6), 1282-1289 (2005).
4. Ruiz-del-Arbol, L., Monescillo, A., Arocena, C., Valer, P., Gines, P., Moreira, V., María Milicua, J., Jiménez, W. and Arroyo, V., Circulatory function and hepatorenal syndrome in cirrhosis. *Hepatology*, **42**(2), 439-447 (2005).
5. Davenport, A., Ahmad, J., Al-Khafaji, A., Kellum, J.A., Genyk, Y.S. and Nadim, M.K. Medical management of hepatorenal syndrome. *Nephrology Dialysis Transplantation*, **27**(1), 34-41 (2012).
6. Al-Najjar, A.H., Ayob, A.R. and Awad, A.S. Role of Lactoferrin in Treatment of Bile Duct Ligation-Induced Hepatic Fibrosis in Rats: Impact on Inflammation and TGF-β1/Smad2/α SMA Signaling Pathway. *Journal of Clinical and Experimental Hepatology*, **13**(3), 428-436 (2023).
7. Tag, C.G., Sauer-Lehnen, S., Weiskirchen, S., Borkham-Kamphorst, E., Tolba, R.H., Tacke, F. and Weiskirchen, R. Bile Duct Ligation in Mice: Induction of Inflammatory Liver Injury and Fibrosis by Obstructive Cholestasis. *Journal of Visualized Experiments*, **96** , e52438 (2015).

8. Liedtke, C., Luedde, T., Sauerbruch, T., Scholten, D., Streetz, K., Tacke, F., Tolba, R., Trautwein, C., Trebicka, J. and Weiskirchen, R., Experimental liver fibrosis research: update on animal models, legal issues and translational aspects. *Fibrogenesis and Tissue Repair*, **6**(1), 1-25 (2013).

9. Svegliati-Baroni, G., Ridolfi, F., Hannivoort, R., Saccomanno, S., Homan, M., De Minicis, S., Jansen, P.L., Candelaresi, C., Benedetti, A. and Moshage, H., Bile acids induce hepatic stellate cell proliferation via activation of the epidermal growth factor receptor. *Gastroenterology*, **128**(4), 1042-1055 (2005).

10. Farnaud, S., and Evans, R.W. Lactoferrin—a multifunctional protein with antimicrobial properties. *Molecular Immunology*, **40**(7), 395-405 (2003).

11. Berlutti, F., Morea, C., Battistoni, A., Sarli, S., Cipriani, P., Superti, F., Ammendolia, M.G. and Valenti, P., Iron Availability Influences Aggregation, Biofilm, Adhesion and Invasion of Pseudomonas Aeruginosa and Burkholderia Cenocepacia. *International Journal of Immunopathology and Pharmacology*, **18**(4), 661-670 (2005).

12. Levay, P.F., Viljoen M. Lactoferrin: a general review. *Haematologica*, **80**(3), 252-267 (1995).

13. Farid, A.S., El Shemy, M.A., Nafie, E., Hegazy, A.M. and Abdelhiee, E.Y. Anti-inflammatory, anti-oxidant and hepatoprotective effects of lactoferrin in rats. *Drug and Chemical Toxicology*, **44**(3), 286-293 (2021).

14. Wang, B., Timilsena, Y.P., Blanch, E. and Adhikari, B. Lactoferrin: Structure, function, denaturation and digestion. *Critical Reviews in Food Science and Nutrition,* **59**(4), 580-596 (2019).

15. Artym, J. and Zimecki, M. Milk-derived proteins and peptides in clinical trials. *Advances in Hygiene and Experimental Medicine*, **67**, 800-816 (2013).

16. Mayadas, T.N., Cullere, X. and Lowell, C.A. The multifaceted functions of neutrophils. *Annual Review of Pathology*, **9**, 181-218 (2014).

17. Bukowska-Ośko, I., Popiel, M. and Kowalczyk, P. The Immunological Role of the Placenta in SARS-CoV-2 Infection-Viral Transmission, Immune Regulation, and Lactoferrin Activity. *International Jurnal of Molecular Sciences,* **22**(11), 5799 (2021).

18. Chodaczek, G., Saavedra-Molina, A., Bacsi, A., Kruzel, M., Sur, S. and Boldogh, I. Iron-mediated dismutation of superoxide anion augments antigen-induced allergic inflammation: effect of lactoferrin. *Advances in Hygiene and Experimental Medicine*, **61,** 268-276 (2007).

19. Yin, H., Cheng, L., Holt, M., Hail, N., Jr., Maclaren R. and Ju, C. Lactoferrin protects against acetaminophen-induced liver injury in mice. *Hepatology*, **51**(3), 1007-1016 (2010).

20. Vesce, F., Giugliano, E., Bignardi, S., Cagnazzo, E., Colamussi, C., Marci, R., Valente, N., Seraceni, S., Maritati, M. and Contini, C., Vaginal Lactoferrin Administration before Genetic Amniocentesis Decreases Amniotic Interleukin-6 Levels. *Gynecologic and Obstetric Investigation*, **77**(4), 245-249 (2014).

21. Tung, Y-T., Chen, H-L., Yen, C-C., Lee, P-Y., Tsai, H-C., Lin, M-F. and Chen, C-M. Bovine lactoferrin inhibits lung cancer growth through suppression of both inflammation and expression of vascular endothelial growth factor. *Journal of Dairy Science,* **96**(4), 2095-2106 (2013).

22. Hessin, A., Hegazy, R., Hassan, A., Yassin, N. and Kenawy, S. Lactoferrin Enhanced Apoptosis and Protected Against Thioacetamide-Induced Liver Fibrosis in Rats. *Open Access Maced. J. Med. Sci.*, **3**(2), 195-201(2015).

23. Flecknell, P. *Laboratory animal anaesthesia*: Academic press*,* (2015).

24. Elsaied, N., Samy, A., Mosbah, E. and Zaghloul, A., Induction of Surgical Obstructive Cholestasis in rats: morphological, biochemical and immunohistochemical changes. *Mansoura Veterinary Medical Journal*, **21**(3), 107-115 (2020).

25. Cooper, D.M., Hoffman, W., Tomlinson, K. and Lee, H-Y. Refinement of the dosage and dosing schedule of ketoprofen for postoperative analgesia in Sprague-Dawley rats. *Lab. Animal,* **37**(6), 271-275 (2008).

26. Bancroft, J.D., Layton, C. and Suvarna, S.K. *Bancroft's theory and practice of histological techniques,* Churchill Livingstone Elsevier. (2013).

27. Thefeld Wea. *Dtsh.Med.wschr*, **99**, 343 (1994).

28. Tietz, N.W. *Fundamentals of clinical chemistry WB Saunders Co*. Philadelphia PA.,47 (1976).

29. Burtis CA, Ashwood ER, Tietz NW. *Tietz textbook of clinical chemistry* (1999).

30. Venter, C., Oberholzer, H. M., Cummings, F. R., & Bester, M. J. Effects of metals cadmium and chromium alone and in combination on the liver and kidney tissue of male Spraque-Dawley rats: An ultrastructural and electron-energy-loss spectroscopy investigation. *Microscopy Research and Technique*, **80**(8), 878-888 (2017).

31. Razali, N.M. and Wah, Y.B. Power comparisons of shapiro-wilk, kolmogorov-smirnov, lilliefors and anderson-darling tests. *Journal of Statistical Modeling and Analytics*, **2**(1), 21-33 (2011).

32. S. A. S. Institute. *SAS/OR 9.3 User's Guide: Mathematical Programming Examples*, SAS institute, (2012).

33. Oberti, F., Vuillemin, E., Fort, J. and Cales, P. Experimental models of portal hypertension. *Gastroenterologie Clinique et biologique*, **24**(10), 896-901 (2000).

34. Pereira, R.M., dos Santos, R.A., Oliveira, E.A., Leite, V.H., Dias, F.L., Rezende, A.S., Costa, L.P., Barcelos, L.S., Teixeira, M.M. and e Silva, A.C.S., Development of hepatorenal syndrome in bile duct ligated rats. *World Journal of gGastroenterology*, **14**(28), 4505-4511 (2008).

35. Poo, J.L., Estanes, A., Pedraza-Chaverri, J., Cruz, C., Perez, C., Huberman, A. and Uribe, M. Chronology of portal hypertension, decreased sodium excretion, and activation of the renin-angiotensin system in experimental biliary cirrhosis. *Revista de Investigacion Clinica; Organo del Hospital de Enfermedades de la Nutricion,* **49**(1),15-23 (1997).

36. Ishikado, A., Imanaka, H., Takeuchi, T., Harada, E. and Makino, T. Liposomalization of Lactoferrin Enhanced It's Anti-inflammatory Effects via Oral Administration. *Biological and Pharmaceutical Bulletin*, **28**(9),1717-1721(2005).

37. Aoyama, Y., Naiki-Ito, A., Xiaochen, K., Komura, M., Kato, H., Nagayasu, Y., Inaguma, S., Tsuda, H., Tomita, M., Matsuo, Y. and Takiguchi, S., Lactoferrin Prevents Hepatic Injury and Fibrosis via the Inhibition of NF-κB Signaling in a Rat Non-Alcoholic Steatohepatitis Model. *Nutrients*, **14**(1), 42 (2021).

38. Tung, Y-T., Tang, T-Y., Chen, H-L., Yang, S-H., Chong, K-Y., Cheng, W.T.K. and Chen, C-M. Lactoferrin protects against chemical-induced rat liver fibrosis by inhibiting stellate cell activation. *Journal of Dairy Science*, **97**(6), 3281-3291 (2014).

39. Bayoumi, Y., Metwally, E., El Nagar, E.A., Abdel Razik, W., El Seddawy, N. and Gomaa, M. Hepatorenal Syndrome in Dogs with Experimental Extrahepatic Cholestasis. *Zagazig Veterinary Journal*, **48**(1), 12-22 (2020).

40. Wang, L. and Yu, W-F. Obstructive jaundice and perioperative management. *Acta Anaesthesiologica Taiwanica,* **52**(1), 22-29 (2014).

41. Ganjalikhan-Hakemi, S., Asadi-Shekaari, M., Pourjafari, F., Asadikaram, G. and Nozari, M. Agmatine improves liver function, balance performance, and neuronal damage in a hepatic encephalopathy induced by bile duct ligation. *Brain and Behaviour,* **13**(9), e3124-e (2023).

42. Pan, P.H., Wang, Y.Y., Lin, S.Y., Liao, S.L., Chen, Y.F., Huang, W.C., Chen, C.J. and Chen, W.Y., Plumbagin ameliorates bile duct ligation-induced cholestatic liver injury in rats. *Biomedicine & Pharmacotherapy,* **151**, 113133 (2022).

43. Ede, S., Özbeyli, D., Erdoğan, Ö., Çevik, Ö., Kanpalta, F., Ercan, F., Yanardağ, R., Saçan, Ö., Ertik, O., Yüksel, M. and Şener, G., Hepatoprotective effects of parsley (Petroselinum Crispum) extract in rats with bile duct ligation. *Arab Journal of Gastroenterology*, **24**(1), 45-51 (2023).

44. Nimbalkar, V. and Vyawahare, N., L-carnitine ameliorates bile duct ligation induced liver fibrosis via reducing the nitrosative stress in experimental animals: preclinical evidences, *Heliyon*, **7**(11), (2021).

45. Ayob, A., Al-Najjar, A. and Awad, A., Amelioration of Bile Duct Ligation Induced Liver Injury by Lactoferrin: Role of Nrf2/HO-1 Pathway. *Azhar International Journal of Pharmaceutical and Medical Sciences*, **1**(3), 84-90 (2021).

46. Saleh, H., Soliman, A.M., Mohamed, A.S. and Marie, M-A.S. Antioxidant effect of sepia ink extract on extrahepatic cholestasis induced by bile duct ligation in rats. *Biomedical and Environmental Sciences*, **28**(8), 582-594 (2015).

47. Singh, P., Khan, S. and Mittal, R. K. Renal function test on the basis of serum creatinine and urea in type-2 diabetics and nondiabetics. *Bali Medical Journal,* **3**(1), 11 (2014).

48. Shah, N., Dhar, D., El Zahraa Mohammed, F., Habtesion, A., Davies, N.A., Jover-Cobos, M., Macnaughtan Jane, Sharma Vikram, Olde Damink Steven W M , Mookerjee P Rajeshwar and Jalan Rajiv. Prevention of acute kidney injury in a rodent model of cirrhosis following selective gut decontamination is associated with reduced renal TLR4 expression. *Journal of Hepatology*, **56**(5), 1047-1053 (2012).

49. Helal, E.G.E., Abd El-Wahab, S.M., Zedan, G.A. and Sharaf, A.M.M. Effect of Zingiber officinale on fatty liver induced by oxytetracycline in albino rats. *The Egyptian Journal of Hospital Medicine,* **46**(1), 26-42 (2012).

50. Gouma, D.J., Coelho, J.C.U., Fisher, J.D., Schlegel, J.F., Li, Y.F. and Moody, F.G. Endotoxemia after relief of biliary obstruction by internal and external drainage in rats. *The American Journal of Surgery*, **151**(4), 476-479 (1986).

51. Murali, A., Ashok, P. and Madhavan, V., Protective effects of Hemidesmus indicus var. pubescens root extract on paracetamol induced hepatic damage. Spatula DD - *Peer Reviewed Journal on Complementary Medicine and Drug Discovery*, **2**(1), 51 (2012).

52. Esmail, M.M., Saeed, N.M., Michel, H.E. and El-Naga , R.N. The ameliorative effect of niclosamide on bile duct ligation induced liver fibrosis via suppression of NOTCH and Wnt pathways. *Toxicology Letters*, **347**, 23-35 (2021).

53. Itha, S. and Aggarwal, R. Profile of Liver Involvement among Adult Patients in Dengue Virus Infection. *Official journal of the American College of Gastroenterology*, **100**, S116 (2005).

54. Fahmy, R. Antioxidant effect of the Egyptian freshwater Procambarus clarkii extract in rat liver and erythrocytes. *African Journal of Pharmacy and Pharmacology,* **5**(6), 776-785 (2011).

55. Ommati, M.M., Farshad, O., Mousavi, K., Taghavi, R., Farajvajari, S., Azarpira, N., Moezi, L. and Heidari, R., Agmatine alleviates hepatic and renal injury in a rat model of obstructive jaundice. *PharmaNutrition*, **13**, 100212 (2020).

56. Kargar, A., Mohammadi, F., Amirizadeh, M., Hallajbashi, N., Kargar, F. and Mohammadi, H. Investigating the Protective Effect of Ellagic Acid on Cholemic Nephropathy in Cholestatic Rats. *Archives of Neuroscience*, **11**(1), e141082 (2024).

57. Atwa, A., Hegazy, R., Mohsen, R., Yassin, N. and Kenawy, S. Protective Effects of the Third Generation Vasodilatory Beta - Blocker Nebivolol against D-Galactosamine - Induced Hepatorenal Syndrome in Rats. *Open Access Maced. J. Med. Sci.*, **5**(7), 880-892 (2017).

58. Javlé, P., Yates, J., Kynaston, H.G., Parsons, K.F. and Jenkins, S.A. Hepatosplanchnic haemodynamics and renal blood flow and function in rats with liver failure. *Gut*, **43**(2), 272-279 (1998).

59. Saracyn, M., Patera, J., Kocik, J., Brytan, M., Zdanowski, R., Lubas, A., Kozłowski, W. and Wańkowicz, Z., Strain of experimental animals and modulation of nitric oxide pathway: their influence on development of renal failure in an experimental model of hepatorenal syndrome. *Arch. Med. Sci.*, **8**(3), 555-562 (2012).

60. Hsu, Y-H., Chiu, I.J., Lin, Y-F., Chen, Y-J., Lee, Y-H. and Chiu, H-W. Lactoferrin Contributes a Renoprotective Effect in Acute Kidney Injury and Early Renal Fibrosis, *Pharmaceutics*, **12**(5), 434 (2020).

61. Woolbright, B.L., Antoine, D.J., Jenkins, R.E., Bajt, M.L., Park, B.K. and Jaeschke, H. Plasma biomarkers of liver injury and inflammation demonstrate a lack of apoptosis during obstructive cholestasis in mice. *Toxicology and applied pharmacology,* **273**(3), 524-531 (2013).

62. Mandorfer, M. and Hecking, M. The Renaissance of Cholemic Nephropathy: A Likely Underestimated Cause of Renal Dysfunction in Liver Disease. *Hepatology*, **69**(5), 1858-1860 (2019).

63. Wijdicks, E.F.M. Hepatic Encephalopathy. *New England Journal of Medicine*, **375**(17),1660-1670 (2016) .

64. Al-Okbi, S.Y., Mohamed, D.A., Hamed, T.E., Mohamed, M.S., El-Sayed, E.M. and Mabrok, H.B. Prevention of hepatorenal syndrome by green tea, branched chain amino acids and mannitol in rat model. *Research Journal of Pharmaceutical Biological and Chemical Sciences*, **7**(3), 1852-1864 (2016).

65. Elnagar M, Mahmoud Y, Mohamed M. Aspartic acid ameliorates cholestasis in bile duct-ligated rats. *Egyptian Journal of Histology*, **46**(4), 26(2022).

66. Ertor, B., Topaloglu, S., Calik, A., Cobanoglu, U., Ahmetoglu, A., Ak, H., Karabulut, E. and Arslan, M.K., The effects of bile duct obstruction on liver volume: an experimental study. ISRN Surg, **2013**, 156347 (2013).

67. Heidari, R., Mohammadi, H., Ghanbarinejad, V., Ahmadi, A., Ommati, M.M., Niknahad, H., Jamshidzadeh, A., Azarpira, N. and Abdoli, N., Proline supplementation mitigates the early stage of liver injury in bile duct ligated rats. *Journal of Basic and Clinical Physiology and Pharmacology*, **30**(1), 91-101(2018).

68. Ramm, G.A., Carr, S.C., Bridle, K.R., Li, L., Britton, R.S., Crawford, D.H., Vogler, C.A., Bacon, B.R. and Tracy Jr, T.F., Morphology of liver repair following cholestatic liver injury: resolution of ductal hyperplasia, matrix deposition and regression of myofibroblasts Note. *Liver*, **20**(5), 387-396 (2000).

69. Slott, P.A., Liu, M.H. and Tavoloni, N. Origin, pattern, and mechanism of bile duct proliferation following biliary obstruction in the rat. *Gastroenterology*, **99**(2), 466-477 (1990).

70. Arya, A., Azarmehr, N. and Mansourian, M., Doustimotlagh AH. Inactivation of the superoxide dismutase by malondialdehyde in the nonalcoholic fatty liver disease: a combined molecular docking approach to clinical studies. *Archives of Physiology and Biochemistry,* **127**(6), 557-564 (2019).

71. Tahan, G., Akin, H., Aydogan, F., Ramadan, S.S., Yapicier, O., Tarcin, O., Uzun, H., Tahan, V. and Zengin, K., Melatonin ameliorates liver fibrosis induced by bile-duct ligation in rats. *Canadian Journal of Surgery (Journal canadien de chirurgie)*, **53**(5), 313-318 (2010).

72. Amália, P.M., Possa, M.N., Augusto, M.C. and Francisca, L.S. Quercetin Prevents Oxidative Stress in Cirrhotic Rats. *Digestive Diseases and Sciences*, **52**(10), 2616-2621 (2007).

73. Tieppo, J., Vercelino, R., Dias, A.S., Marroni, C.A. and Marroni, N. Common bile duct ligation as a model of hepatopulmonary syndrome and oxidative stress. *Arq. Gastroenterol.,* **42**(4), 244-248 (2005).

74. Ferrari, R..S., Tieppo, M., Rosa, D.Pd., Forgiarini, Jr. L.A., Dias, A.S. and Marroni, N.P. Lung and liver changes due to the induction of cirrhosis in two experimental models. *Arquivos de Gastroenterologia*, **50**(3), 208-213 (2013).

75. Sanchez-Valle, V.C., Chavez-Tapia, N., Uribe, M. and Mendez-Sanchez, N. Role of Oxidative Stress and Molecular Changes in Liver Fibrosis - A Review, *Current Medicinal Chemistry,* **19**(28), 4850-4860 (2012).

76. Jamshidzadeh, A., Heidari, R., Latifpour, Z., Ommati, M.M., Abdoli, N., Mousavi, S., Azarpira, N., Zarei, A., Zarei, M., Asadi, B. and Abasvali, M., Carnosine ameliorates liver fibrosis and hyperammonemia in cirrhotic rats. *Clinics and Research in Hepatology and Gastroenterology*, **41**(4), 424-34 (2017).

77. Krones, E., Eller, K., Pollheimer, M.J., Racedo, S., Kirsch, A.H., Frauscher, B., Wahlström, A., Ståhlman, M., Trauner, M., Grahammer, F. and Huber, T.B., NorUrsodeoxycholic acid ameliorates cholemic nephropathy in bile duct ligated mice. *Journal of Hepatology*, **67**(1), 110-119 (2017).

78. Ommati, M.M., Hojatnezhad, S., Abdoli, N., Manthari, R.K., Jia, Z., Najibi, A., Akbarizadeh, A.R., Sadeghian, I., Farshad, O., Azarpira, N. and Niknahad, H., Pentoxifylline mitigates cholestasis-related cholemic nephropathy. *Clin. Exp. Hepatol.,* **7**(4), 377-389 (2021).

79. Angeli, P., Garcia-Tsao, G,. Nadim, M.K. and Parikh, C.R. News in pathophysiology, definition and classification of hepatorenal syndrome: A step beyond the International Club of Ascites (ICA) consensus document. *Journal of Hepatology*, **71**(4), 811-822 (2019).

80. Galle J., Heermeier, K. and Wanner, C. Atherogenic lipoproteins, oxidative stress, and cell death. *Kidney International,* **56**, S62-S5 (1999).

81. Vaziri, N.D. and Norris, K.C. Reasons for the lack of salutary effects of cholesterol-lowering interventions in end-stage renal disease populations. *Blood Purification*, **35**(1-3), 31-36 (2013).

82. Shah, S.V. Role of iron in progressive renal disease. *American Journal of Kidney Diseases*, **37**(1), S30-S3 (2001).

83. Zheng, J., Xie, Y., Li, F., Zhou, Y., Qi, L., Liu, L. and Chen, Z., Lactoferrin improves cognitive function and attenuates brain senescence in aged mice. *Journal of Functional Foods*, **65**, 103736 (2020).

84. Handelman, G.J., Walter, M.F., Adhikarla, R., Gross, J., Dallal, G.E., Levin, N.W. and Blumberg, J.B. Elevated plasma F2-isoprostanes in patients on long-term hemodialysis. *Kidney International,* **59**(5), 1960-1966 (2001).

85. van Slambrouck, C.M., Salem, F., Meehan, S.M. and Chang, A. Bile cast nephropathy is a common pathologic finding for kidney injury associated with severe liver dysfunction. *Kidney International,* **84**(1),192-197 (2013).

86. Bairaktari, E. Partially reversible renal tubular damage in patients with obstructive jaundice. *Hepatology*, **33**(6), 1365-1369 (2001).

87. Wadei, H.M., Mai, M.L., Ahsan, N. and Gonwa, T.A. Hepatorenal Syndrome. *Clinical Journal of the American Society of Nephrology*, **1**(5), 1066-1079 (2006).

88. Ortiz, M.C., Manriquez, M.C., Nath, K.A., Lager, D.J., Romero, J.C. and Juncos, L.A. Vitamin E prevents renal dysfunction induced by experimental chronic bile duct ligation. *Kidney Int.*, **64**(3), 950-961 (2003).

89. Zhang, J., Zhang, Q., Wang, Y., Li, J., Bai, Z., Zhao, Q., Wang, Z., He, D., Zhang, J. and Chen, Y., Toxicities and beneficial protection of H 2 S donors based on nonsteroidal anti-inflammatory drugs. *MedChemComm*, **10**(5), 742-756 (2019).

90. Wang, W., Yan, J., Wang, H., Shi, M., Zhang, M., Yang, W., Peng, C. and Li, H., Rapamycin ameliorates inflammation and fibrosis in the early phase of cirrhotic portal hypertension in rats through inhibition of mTORC1 but not mTORC2. *PloS one*, **9**(1), 83908 (2014).

91. Deroee, A.F., Nezami, B.G., Mehr, S.E., Hosseini, R., Salmasi, A.H., Talab, S.S., Jahanzad, I. and Dehpour, A.R.,. Cholestasis induced nephrotoxicity: the role of endogenous opioids. *Life Sciences*, **86**(13-14), 488-492 (2010).

92. Melvin, T., Burke, B., Michael, A.F. and Kim, Y., Experimental IgA nephropathy in bile duct ligated rats. *Clinical Immunology and Immunopathology*, **27**(3), 369-377 (1983).

دراسات باثولوجية وكيميائية حيوية حول المتلازمة الكبدية الكلوية الناجمة عن ربط القناة الصفراوية في الفئران البيضاء

ندى نبيل مصطفى ابراهيم خليل[1] ، ولاء فكري عبدالوهاب حسن[1] ، الاء سامى السيد عبد الخالق[2] و أحمد فوزي محمد الشايب [3]

[1] قسم الباثولوجيا - كلية الطب البيطري - جامعة المنصورة - المنصورة - مصر .

[2] قسم التخدير والأشعة - كلية الطب البيطري - جامعة المنصورة - المنصورة - مصر .

[3] قسم الباثولوجيا- كلية الطب البيطري - الجامعة المصرية الصينية - القاهرة - مصر.

الملخص

تعرف المتلازمة الكبدية الكلوية أنها شكل من أشكال الفشل الكلوي الثانوي ، الذي يحدث في المراحل المتأخرة من أمراض الكبد المزمنة. وتنبع أهميتها من أنها تتميز بأقل معدل بقاء على قيد الحياة. تهدف هذه الدراسة إلى معرفة الدور العلاجي لعقار للاكتوفيرين ضد مضاعفات التليف الكبدي المرتبط بربط القناة المرارية في الجرذان كنموذج تجريبى لهذه الدراسة.

أجريت هذه التجربة على 36 ذكراً بالغاً من الجرذان بوزن (250 - 300 جم) وتراوحت أعمارهم بين (5-6) أسابيع. تم تقسيم هذه الجرذان عشوائيا الى أربع مجموعات؛ المجموعة الأولى وهى مجموعة السيطرة وعددها 6، تلقت الجرذان فى هذه المجموعة جرعة يومية من الماء المقطر عن طريق انبوبة معدية بمعدل (100 مل/كجم) لمدة 4 أسابيع متتالية، المجموعة الثانية وهى التى تلقت عقار اللاكتوفرين فقط وعددها 6 ، تلقت الجرذان فيها جرعة فموية من اللاكتوفيرين بمعدل (300 مجم / كجم) عن طريق أنانبيب معدية يوميا لمدة 4 أسابيع متتالية، المجموعة الثالثة؛ وهى مجموعة الربط وعددها 12، خضعت تلك المجموعة لعملية ربط القناة المرارية ربط مزدوج فقط دون تلقى أى علاج، المجموعة الرابعة و عددها 12، فى هذه المجموعة تم ربط القناة المرارية في الجرذان ربط مزدوج ثم تلقت العلاج بعقار اللاكتوفرين عن طريق انابيب معدية بدءا من اليوم التالى للجراحة واستمرت على العلاج يوميا لمدة 4 أسابيع متتالية. أثبتت الدراسة الحالية أن العلاج بعقار اللاكتوفرين أظهر تحسنًا جليا في العلامات السريرية ، التحليلات الكيميائية الحيوية ، الفحوصات النسيجية المرضية والفحص المجهرى الالكترونى للكبد والكلى فى الجرذان التى خضعت لربط القناة المرارية مع تلقى العلاج من اليوم التالى للجراحة مقارنة بمجموعة الربط التى لم تتلقى العلاج. ونستخلص من هذا أن عقار اللاكتوفرين يلعب دورًا هاما في علاج التليف الكبدي وما يرتبط به من مضاعفات بما في ذلك المتلازمة الكبدية الكلوية وذلك من خلال الخصائص التى يتمتع بها كمضاد للأكسدة.

الكلمات الدالة: اللاكتوفرين، المتلازمة الكبدية الكلوية، تليف الكبد، الجرذان، ربط القناة المرارية.